Universal window for two-dimensional critical exponents

2008 J. Phys.: Condens. Matter 20 275233

(http://iopscience.iop.org/0953-8984/20/27/275233)

J. Phys.: Condens. Matter **20** (2008) 275233 (15pp) doi:10.1088/0953-8984/20/27/275233

Universal window for two-dimensional critical exponents

A Taroni[1,4], S T Bramwell[2,1] and P C W Holdsworth[3]

[1] Department of Chemistry, University College London, 20 Gordon Street, London WC1H 0AJ, UK
[2] London Centre for Nanotechnology, 17-19 Gordon Street, London WC1H 0AH, UK
[3] Université de Lyon, Laboratoire de Physique, École Normale Supérieure de Lyon, 46 Allée d'Italie, 69364 Lyon cedex 07, France

E-mail: andrea.taroni@fysik.uu.se, s.t.bramwell@ucl.ac.uk and peter.holdsworth@ens-lyon.fr

Received 4 February 2008, in final form 26 March 2008
Published 6 June 2008
Online at stacks.iop.org/JPhysCM/20/275233

Abstract
Two-dimensional condensed matter is realized in increasingly diverse forms that are accessible to experiment and of potential technological value. The properties of these systems are influenced by many length scales and reflect both generic physics and chemical detail. To unify their physical description is therefore a complex and important challenge. Here we investigate the distribution of experimentally estimated critical exponents, β, that characterize the evolution of the order parameter through the ordering transition. The distribution is found to be bimodal and bounded within a window $\sim 0.1 \leqslant \beta \leqslant 0.25$, facts that are only in partial agreement with the established theory of critical phenomena. In particular, the bounded nature of the distribution is impossible to reconcile with the existing theory for one of the major universality classes of two-dimensional behaviour—the XY model with four-fold crystal field—which predicts a spectrum of non-universal exponents bounded only from below. Through a combination of numerical and renormalization group arguments we resolve the contradiction between theory and experiment and demonstrate how the 'universal window' for critical exponents observed in experiment arises from a competition between marginal operators.

(Some figures in this article are in colour only in the electronic version)

1. Introduction

New types of two-dimensional systems on which meaningful physical experiments can be performed include optical lattices of trapped atomic gases [1], magnetic surfaces [2] and 'δ-doped' magnetic layers [3]. These add to a list of well established two-dimensional systems that includes ultrathin magnetic films [4], atomic monolayers (both physi- and chemisorbed) [5–8], crystalline surfaces [9], superconducting layers [10] and arrays of interacting Josephson junctions [11]. Recent theoretical developments on the concept of 'extended universality' [12], the effects of finite size [13, 14] and the dipolar interaction [15, 16] should be particularly relevant to understanding experiments on these systems, both old and new.

[4] Present address: Department of Physics, Uppsala University, Box 530, 751 21 Uppsala, Sweden.

The key experiment on two-dimensional systems is to test the existence and temperature dependence of a magnetic or crystalline order parameter $m(T)$. In cases where m can be measured experimentally (which excludes, for example, superfluid films [7]), this is invariably found to approximate a power law over a certain range of temperature: $m \sim (T_c - T)^{\beta}$, where T_c is the transition temperature. Theory predicts a limited number of possibilities for the value of the exponent β, as dictated by the universality class of the system. In two dimensions crystal symmetries and consequent universality classes are relatively few. We show here that the Ising, XY and XY with four-fold crystal field anisotropy (XYh_4) are the three main experimentally relevant classes. The three- and four-state Potts models provide additional universality classes observed in experiments on adsorbed gaseous monolayers [17, 18] and surface reconstruction [9]. For the Ising, three- and four-state Potts models, $\beta = \frac{1}{8}, \frac{1}{9}, \frac{1}{12}$ respectively. For the XY model, one

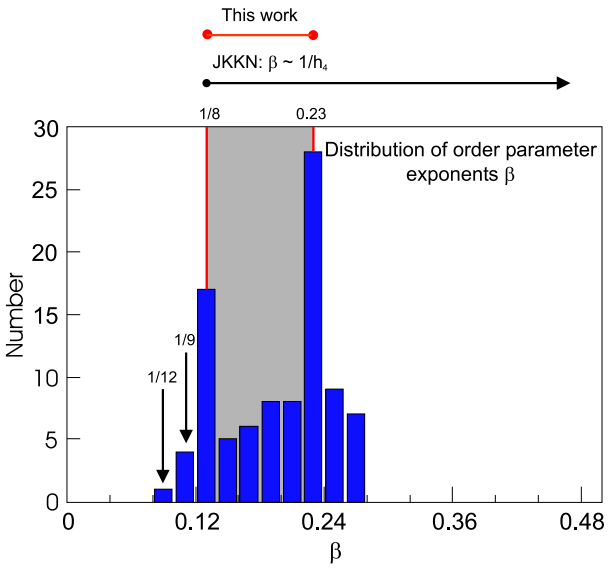

Figure 1. Histogram of β values for all two-dimensional systems reported in tables A.1–A.3. The universal window is highlighted by the grey shading. Criteria for inclusion in the data set are discussed in the appendix, and the occurrence of systems with exponent values outside the window is discussed in section 1.

expects $\tilde{\beta} = 0.23$, a universal number that arises in the finite size scaling at the Kosterlitz–Thouless–Berezinskii (KTB) phase transition [19, 20], though not a conventional critical exponent [21]. For XYh_4, theory predicts a continuously variable critical exponent $\beta \propto 1/h_4$ and thus a continuous spectrum of values when sampled over many real systems (see [22, 23] and this work).

We have tested these ideas by means of an extensive survey of experimental two-dimensional critical exponents, including data for magnetic ultrathin films, layered magnets that exhibit a temperature regime of two-dimensional behaviour [24–27], order–disorder transitions in adsorbed gaseous monolayers [17, 18], and surface reconstructions [9]. The results are presented in figure 1 and in the appendix. As observed previously on more limited data sets [4, 21, 28, 29], the distribution of β is distinctly bimodal, with strong peaks at $\beta = 0.12$ and 0.23, as expected for the Ising and XY models. In several cases ideal Ising [24, 30] and XY [25–27, 31, 32] behaviour has been confirmed in great detail by measuring thermodynamic quantities other than the magnetization. Likewise there is compelling evidence for Potts universality in several non-magnetic systems [17, 18, 33, 34, 9] ($\beta = \frac{1}{8}, \frac{1}{9}$ on the histogram in figure 1). However, the XYh_4 universality is more elusive. Of particular relevance to the present discussion are the ferromagnetic monolayer Fe/W(100) [32] and the layered ferromagnets Rb_2CrCl_4 [25] and K_2CuF_4 [26], easy plane systems which have been shown to exhibit the full range of ideal XY behaviour despite their four-fold symmetry. Another very well characterized easy plane system with a four-fold crystal field is the layered antiferromagnet K_2FeF_4 [31], but this is not XY-like, with $\beta = 0.15$ intermediate between the XY and Ising values. Claims for XYh_4 universality have been made for the ferromagnetic films Fe/[Au or Pd](100) [35], characterized only to a limited extent, as well as the order–disorder transitions of H/W(011) [36] and O/Mo(110) [37], for which full sets of critical exponents are available. The behaviour of these candidates for XYh_4 is seen to fall into two categories, which on closer inspection appear to be related to the strength of h_4: those with weak h_4 are XY-like with $\beta \approx 0.23$, while those with stronger h_4 have exponents in between the XY and Ising limits, $0.125 \leqslant \beta \leqslant 0.23$. Most strikingly, there is no experimental evidence of the divergence of the exponent β implied by $\beta \propto 1/h_4$. Instead, most experimental data that cannot be ascribed to the Potts classes lie in a 'universal window', bounded by the Ising and XY values. There are exceptions at the upper bound where crossover to three-dimensional behaviour may increase the value of β upwards from 0.23 [21, 38]. However, it is clear from the histogram that the majority of systems are indeed encompassed in a limited range between the Ising and XY values.

The rest of the paper is structured as follows. In the next section we review the symmetries and universality classes appearing in experimental two-dimensional systems. In section 3 we calculate the critical exponents for the XYh_4 universality class from the renormalization group starting from the generalized Villain Hamiltonian. The calculation predicts that the value of β should be non-universal, varying inversely with the crystal field strength, for weak perturbations. In section 4 we analyse numerical data for different crystal fields. Our simulation data are consistent with experiment, as shown in figure 1, but in flagrant disagreement with the predictions of section 3. A resolution of this disagreement is proposed, which is examined in detail in the subsequent discussion. Section 5 makes head to head comparisons between materials believed to correspond to the strong and weak crystal field case. We argue that, in the case of antiferromagnets, quantum fluctuations lead to spin dimensional reduction and an increase in the effective crystal field strength, compared with similarly parametrized ferromagnets and classical systems. Section 6 deals with other critical exponents and discusses the experimental consequences of finite size corrections to the thermodynamic limit.

2. Universality classes in two dimensions

Before we address the main question of why the universal window exists, it is relevant to specify the occurrence and relationships between two-dimensional universality classes. Considering first magnetic degrees of freedom, we ignore the possibility of truly Heisenberg behaviour, remarking that the broken translational symmetry inherent to layers or surfaces, combined with a condition of crystal periodicity, means all real systems have at least one p-fold axis, which necessarily introduces relevant perturbations. Thus, although pure Heisenberg behaviour may be observable over a restricted temperature range [39, 40], it must give way to behaviour characteristic of the perturbations at temperatures near to the phase transition. These perturbations take the form of axial anisotropy (either easy axis or easy plane) and p-fold in-plane anisotropy ($p = 1, 2, 3, 4$ and

Table 1. Classification of continuous transitions which can be observed in two-dimensional magnetic systems and in structural order–disorder transitions on surfaces. • indicates the occurrence of a particular universality class, whereas × indicates its absence. The special case of the square lattice dipolar system is discussed in the text.

Universality class	Magnetic systems	Adsorbed systems
Ising	•	•
XY	•	•
XYh_4	•	•
Three-state Potts	×	•
Four-state Potts	×	•

6). Easy-axis systems are generally Ising-like (despite the fact that the normal to the plane is usually a polar axis) while easy plane systems with $p = 2$–6 should be described by the XYh_p model. XYh_2 is in the Ising class, whereas XYh_3 is in the three-state Potts class, although it is very unlikely in magnetic systems owing to time reversal symmetry (we found no examples). XYh_4 constitutes a universality class distinct from the four-state Potts class, while the phase transition in XYh_6 is in the XY class [22]. Inclusion of the dipolar interaction on lattices other than the square lattice does not add extra universality classes. However, the case of the square lattice must be regarded as an unsolved problem: perturbative calculations [41] and numerical results [42–44] suggest that the square lattice dipolar model belongs to XYh_4, but the renormalization group calculations of Maier and Schwabl indicate a different set of critical exponents [15]. The experimental data considered here are consistent with the former result rather than with the latter, but Maier and Schwabl's prediction could yet be born out on an as yet undiscovered ideal model dipolar system. At least as far as the existing experimental data set is concerned, we conclude that, for magnetic systems, there are only three main universality classes: Ising, XY and XYh_4.

The situation is essentially the same in non-magnetic systems [45, 46] but with the additional possibility of the three- or four-state Potts classes due to competing interactions beyond nearest neighbour [46, 47]. Indeed, Schick [46] used arguments from Landau theory to classify the phase transitions of two-dimensional adsorbed systems into only four classes: the Ising, XYh_4, three- and four-state Potts. This set is supplemented by a chiral three-state Potts class which shares conventional exponents with the pure three-state Potts class [48] (hence for present purposes we shall treat these two cases as a single class). One result of the current work is that the pure XY class is also relevant to order–disorder transitions in adsorbed layers. Combining these observations we have five universality classes for structural systems and three for magnetic systems, as summarized in table 1.

3. Calculation of critical exponents

The relationship between the Ising, XY, XYh_p and clock models may be discussed with reference to the following Hamiltonian:

$$\mathcal{H}_p = -J\sum_{\langle i,j\rangle}\cos(\theta_i-\theta_j)-h_p\sum_i\cos(p\theta_i), \qquad (1)$$

in which the θ_i are the orientations of classical spins of unit length situated on a square lattice with periodic boundary conditions and confined to the XY plane, J is the coupling constant and h_p is the p-fold crystal field. It should be noted that unlike real systems, the lattice symmetry in computer simulations does not constrain the spin symmetry, and consequently the adoption of a square lattice does not restrict the generality of our arguments. In the limit $h_p\to\infty$, the Hamiltonian (1) is called a clock model, since θ_i is restricted to discrete values evenly spaced around a circle: $2\pi(n/p)$, $n = 1,\ldots,p-1$. José, Kadanoff, Kirkpatrick and Nelson (JKKN) [22] have shown that for $p > 4$, h_p is an irrelevant scaling field down to intermediate temperatures, with the result that fluctuations restore the continuous symmetry of the 2dXY model above a threshold temperature, leading to a KTB transition [20] and quasi-long-range order over a finite range of temperature. Recently it has been shown [12] that a similar scenario remains valid even for infinitely strong crystal field strength, with the result that fluctuations restore continuous symmetry for p-state clock models with $p > 4$, although for $4 < p \leqslant 6$ this occurs above the KTB temperature, T_{KT}. For $p = 2$ and 3, h_p is relevant, leading to phase transitions in the Ising and three-state Potts universality class respectively. h_4, on the other hand, is a marginal perturbation [22]. A second-order phase transition is predicted with non-universal critical exponents depending on the field strength. As $h_4\to\infty$, XYh_4 crosses over to the four-state clock model, which is equivalent to two perpendicular Ising models, and the transition falls into the Ising universality class [49]. The non-universal transition for XYh_4 is hence bounded by the Ising universality class for large h_4.

The non-universal exponents of XYh_4 can be calculated analytically within the framework proposed by JKKN. They showed that to describe the evolution of the KTB transition in the presence of a weak p-fold field it is sufficient to replace (1) by the generalized Villain Hamiltonian [22, 50]

$$\frac{\mathcal{H}}{k_{\mathrm{B}}T} = -K\sum_{\langle i,j\rangle}\left[1-\frac{1}{2}(\theta_i-\theta_j-2\pi m_{ij})^2\right]+\sum_i \mathrm{i}pn_i\theta_i + \log(y_0)\sum_i S_R^2+\log(y_p)\sum_i n_i^2, \qquad (2)$$

where $K = J/k_{\mathrm{B}}T$. The integers m_{ij} maintain the periodicity of the original Hamiltonian, for rotations over an angle 2π. S_R is a directed sum of integers m_{ij} around a square plaquette of four sites centred at $\vec{R}$: $S_R = m_{41}+m_{12}-m_{32}-m_{43}$ takes values $S_R = 0, \pm1, \pm2\ldots$ and is therefore a quantum number for a vortex of spin circulation centred on the dual lattice site $\vec{R}$. y_0 is related to the chemical potential μ and fugacity y for the creation of a vortex–anti-vortex pair on neighbouring dual lattice sites: $y = y_0\exp(-\beta\mu)\approx y_0\exp(-\pi^2K/2)$. In the original Villain model $y_0 = 1$ but it is introduced here as a phenomenologically small parameter which is renormalized in the subsequent flows. Similarly y_p is a fugacity for a locking process of spins along one of the p-fold field directions with integer n_i being a measure of the strength of this process at site i. For weak crystal fields, $y_p = \frac{1}{2}\tilde{h}_p$ with $\tilde{h}_p = (h_p/k_{\mathrm{B}}T)$, which reproduces the field contribution to the partition function to leading order in y_p. For strong fields $y_p\to1$ and (2) transforms

into a discrete p-state model. Note, however, that this is not the p-state clock model: although the Villain model maintains the global rotational symmetry it destroys the local O(2) symmetry of the pair interaction. The discrete terms $(\theta_i-\theta_j-2\pi m_{ij})^2$, $\theta_i = (n/p)2\pi$, $n = 0, 1, \ldots, p-1$ hence do not have this symmetry over the interval $-\pi < (\theta_i-\theta_j-2\pi m_{ij}) < \pi$. For $p = 4$ this means that neighbouring spins orientated perpendicularly have an energy less than half that of antiparallel spins and the ordered state has lower lying excitations than the corresponding clock model. It is therefore not clear whether the Villain model falls into the correct universality class in the strong field limit and for quantitative studies one should use Hamiltonian (1) rather than (2).

With y_p set equal to zero, a direct space renormalization analysis for the spin–spin correlation functions resulting from (2) leads to RG flow equations for an effective coupling constant $K_{\rm eff}$ and vortex fugacity, y. For $K_{\rm eff} = 2/\pi$, $y = 0$, the flows yield the KTB transition [51]. In the presence of the p-fold field the flow equations are modified and a third equation is generated [22, 52]. For the explicit case with p=4, these are

$$(K^{-1})' = K^{-1}+4\left(\pi^3 y_0^2 {\rm e}^{-\pi^2 K}-4\pi K^{-2} y_4^2 {\rm e}^{-4K^{-1}}\right)\ln(b) \quad (3a)$$

$$y_0' = y_0+(2-\pi K)\,y_0 \ln(b) \quad (3b)$$

$$y_4' = y_4+\left(2-\frac{4K^{-1}}{\pi}\right)y_4 \ln(b), \quad (3c)$$

where b is the scale factor and where the equations are valid as $b\to 1$. This set of equations has fixed points at $K^* = 2/\pi$, $y_0^* = \pm y_4^*$. We can calculate the linearized transformation matrix evaluated at the fixed point, $*$: $M_{i,j} = \frac{\partial K_i}{\partial K_j}|_*$, where $K_i = K^{-1}$, y_0, y_4.

Solving for the eigenvalues we find

$$\lambda = 1,\ 1+\frac{\alpha}{2}\pm\frac{1}{2}\sqrt{4a^2+\alpha^2}, \quad (4)$$

where $\alpha = 16\pi^2(2\pi-1)\tilde{y}^2{\rm e}^{-2\pi}\ln(b)$, $a^2 = 2\gamma\delta$, $\delta = \frac{4}{\pi}\tilde{y}\ln(b)$, $\gamma = 8\pi^3\tilde{y}{\rm e}^{-2\pi}\ln(b)$, and where $y_0 = y_4 = \tilde{y}$. Writing $\lambda = b^\sigma$ we extract the three scaling exponents. There is one relevant exponent, which is interpreted as $\sigma_1 = 1/\nu$, the exponent taking the coupling constant away from the critical value at the now regular second-order phase transition. There is also one irrelevant variable σ_2, which is interpreted as driving the vortex fugacity to zero. Finally, there is one marginal variable, σ_3, which, as announced, corresponds to the scaling exponent of the four-fold crystal field. Taking $h_4 = 0$ all eigenvalues become marginal, consistent with the particular scaling properties of the 2dXY model. In the small field limit, $\sigma_1 = -\sigma_3 = 4\pi{\rm e}^{-\pi}\tilde{h}_4$ and $\sigma_2 = 0$. This gives the non-universal correlation length exponent [22] $\nu\approx 1.8(k_{\rm B}T_{\rm KT}/h_4)$. The strong field limit, $y_4 = 1$ gives $\nu\approx 0.47$, which should be compared with the exact result for the Ising model, $\nu = 1$. The agreement is poor, as might be expected given the distortion of the four-fold interaction imposed by the Villain model. It is clear from this result that a quantitative calculation for the strong field limit requires a different starting Hamiltonian.

In order to calculate β from the scaling relations [53], a second relevant scaling exponent is required. In this case the anomalous dimension exponent η can be calculated directly from the correlation function [22]. At the KTB transition of the XY model, $\eta = 1/4$, giving the universal value in the effective spin stiffness, $K_{\rm eff} = 2/\pi$. It follows from the scaling relation $2\beta = (d-2+\eta)\nu$ that the finite size scaling exponent $\beta/\nu = 1/8$, as in the Ising model, despite the fact that here the true β and ν are not defined. This is an example of 'weak universality' [54] between the two models. A striking result in the presence of a four-fold field is that η remains unchanged to lowest order in h_4 [22], indicating that a weak universal line extends out from the XY model along the h_4 axis. Here we make the hypothesis that the line extends right to the Ising limit, in which case $\eta = 1/4$ for all h_4. This is clearly a reasonable assumption for the level of calculation made here. It is also an appealing result as other examples of weak universality are far less accessible to experiment [55]. Analysis of the numerical data presented in the next section lends weight to this hypothesis, although the observed behaviour is found to divide into two regimes, depending on the strength of the h_4 field.

From this analysis we therefore predict a range of non-universal magnetization exponents going from

$$\beta\approx\frac{1}{8}\left(\frac{1.8k_{\rm B}T_{\rm KT}}{h_4}\right) \quad (5)$$

for weak field, to $\beta = 1/8$ in the strong field limit. To make quantitative comparison with simulation and experiment we need to estimate β as a function of h_4/J. The critical value $K^* = 2/\pi$ corresponds to a renormalized coupling constant, $J_{\rm eff}$, valid at large length scale such that $k_{\rm B}T_{\rm KT} = \pi J_{\rm eff}/2$. In general $J_{\rm eff} < J$: for the Villain model $k_{\rm B}T_{\rm KT}\approx 1.35J$ [56], while for the XY Hamiltonian (1) $k_{\rm B}T_{\rm KT}/J\approx 0.9$ and is different again for more realistic Hamiltonians. Hence, while we can make a theoretical prediction for the low field behaviour,

$$\beta = \frac{1}{8}\left(\frac{AJ}{h_4}\right), \quad (6)$$

with A a constant of order unity, scaling equation (5) by a factor $k_{\rm B}T_{\rm KT}/J$ will probably not lead to an accurate quantitative estimate for A and the precise value is beyond the scope of the present calculation.

4. Competition with essential finite size effects

The survey of the β values illustrated in figure 1 shows a clear discrepancy between theory presented above and experiment: the large values of β predicted for small h_4 do not appear and the range of values is cut off at $\beta\approx 0.23$. As the latter is an effective exponent characteristic of XY criticality up to a finite length scale, it seems clear that the non-universal critical phenomena are suppressed, for weak field, by the exceptional finite size scaling properties of the pure 2dXY model [21, 57, 58]. This hypothesis can be tested by numerical simulation, in which both h_4 and the system size may be directly controlled.

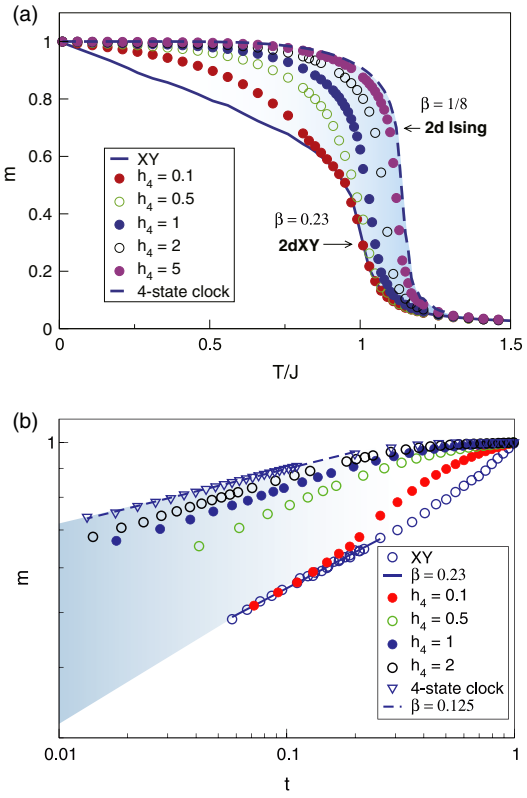

Figure 2. Monte Carlo data for the 2dXY model in the presence of a four-fold crystal field, with $N = 10^4$. Plot (a) displays the magnetization data of the XY model in the presence of increasingly strong anisotropies. Plot (b) displays the same data as a function of reduced temperature t, in a logarithmic scale. In both plots the 'universal window' is highlighted by the (blue) shading.

In a real XY system the relevant length scale will in most cases be less than the physical size of the system: for example, it could be a coherence length controlled by defects or dipolar interactions [59], or, in the case of layered systems, a crossover scale to the third dimension [60, 21]. Thus, although real systems might have, for example, 10^{16} spins, the relevant scale for XY critical behaviour will typically be much smaller and compatible with the scale of Monte Carlo simulations, where the appropriate length scale is simply the system size. This finite length scale gives rise to a finite magnetization that disappears at the rounded KTB transition. As emphasized in [21], this is perfectly consistent with the Mermin–Wagner theorem [61], which proves that the magnetization will be strictly zero in the thermodynamic limit. It is easy to convince oneself that finite size corrections to the thermodynamic limit are important for any physically realizable cut off length scale. The resulting low temperature magnetization is therefore directly relevant for experiment.

In figure 2(a) we show the magnetic order parameter,

$$m = \frac{1}{N}\left\langle \left| \sum_i \mathbf{S}_i \right| \right\rangle,$$

the thermally averaged magnetic moment normalized to unity, versus temperature, with different four-fold field perturbations, for a system with $N = 10^4$ spins. For $h_4 = 0$ the magnetization is characterized by the effective critical exponent, $\tilde{\beta} \approx 0.23$. A finite size analysis of Kosterlitz' renormalization group equations shows that in the region of the transition it approaches a universal number $\tilde{\beta} = 3\pi^2/128 \approx 0.23$, in agreement with both experiment and simulation data, such as that shown here. For weak crystal field, h_4 there is no change in the region of the transition and the magnetization data coincide with the data for zero field [62]. Only for $h_4/J \geqslant 0.5$ do they leave the zero field data through the transition, approaching results for the four-state clock model for large values of h_4/J. In figure 2(b) we show $\log(m)$ against $\log(t)$, where $t = (T - T_c)/T_c$. The transition temperature T_c is calculated from a finite size scaling analysis of the fourth-order Binder cumulant for m [63, 64, 59] and is an estimate of the value in the thermodynamic limit. The slopes, for small t, give a first estimate of the exponent β, indicating that it lies in the interval $1/8 < \beta(h_4) < 0.23$ for all values of h_4, exactly as observed in experiment. The crossover to Ising behaviour is slow: for $h_4/J = 1$, $\beta(h_4) \approx 0.15$ and to approach $\beta \approx 1/8$ requires h_4/J in excess of 5.

Hence the data here, as in previous numerical work [62, 65, 64], show evidence for a finite pocket of XY critical behaviour for small values of h_4. This appears to refute the prediction of JKKN, derived explicitly in the previous section, that the exponents vary continuously with h_4 [65] (see the further discussion below). For intermediate field strengths, however, the non-universal criticality does appear to hold as can be confirmed by a more detailed finite size scaling analysis. The values of β and ν can be estimated more accurately by collapsing data for various system sizes onto the scaling relation $mL^{\beta/\nu} = f(tL^{1/\nu})$, where f is a scaling function. The best data collapses for $h_4/J = 1$ and 2, with T_c in each case fixed from the Binder cumulant calculation, are shown in figure 3. We find $\beta = 0.148(5)$ and $\beta = 0.136(10)$, in good agreement with the values found from figure 2(b), and $\nu = 1.19(4)$, $\nu = 1.09(8)$. The ratio $\beta/\nu = 0.126(4)$ in each case is in agreement with the weak universality hypothesis. Similar results for $h_4/J = 0.5$ can be found in [65]. Although these exponent values are not so different from the Ising model values, the data collapse is less satisfactory when Ising exponents are used.

Further evidence for weak universality at intermediate field strengths can be found from studying the finite size scaling properties of m at the transition. In figure 4 we show $\log(m)$ against $\log(L)$ for $h_4/J = 1$ for a range of temperatures near the transition. At the transition one expects a power law evolution characterized by the finite size scaling exponent $\eta/2 = \beta/\nu$. The best power law occurs at $T_c = 1.010(5)J$, which is the same as the value found from the Binder cumulant method. The scaling exponent $\eta/2 = 0.126(3)$, is the same as that found for the data collapse in figures 3(a) and (b).

This and previous numerical work [62, 65, 64, 66] are consistent with h_4 being marginal. In this case the crossover exponent to the new universality class is zero so crossover occurs, at best on exponentially large length scales, as a result of corrections to scaling [62]. Hence, for small and intermediate crystal field strengths the finite size scaling appears compatible with

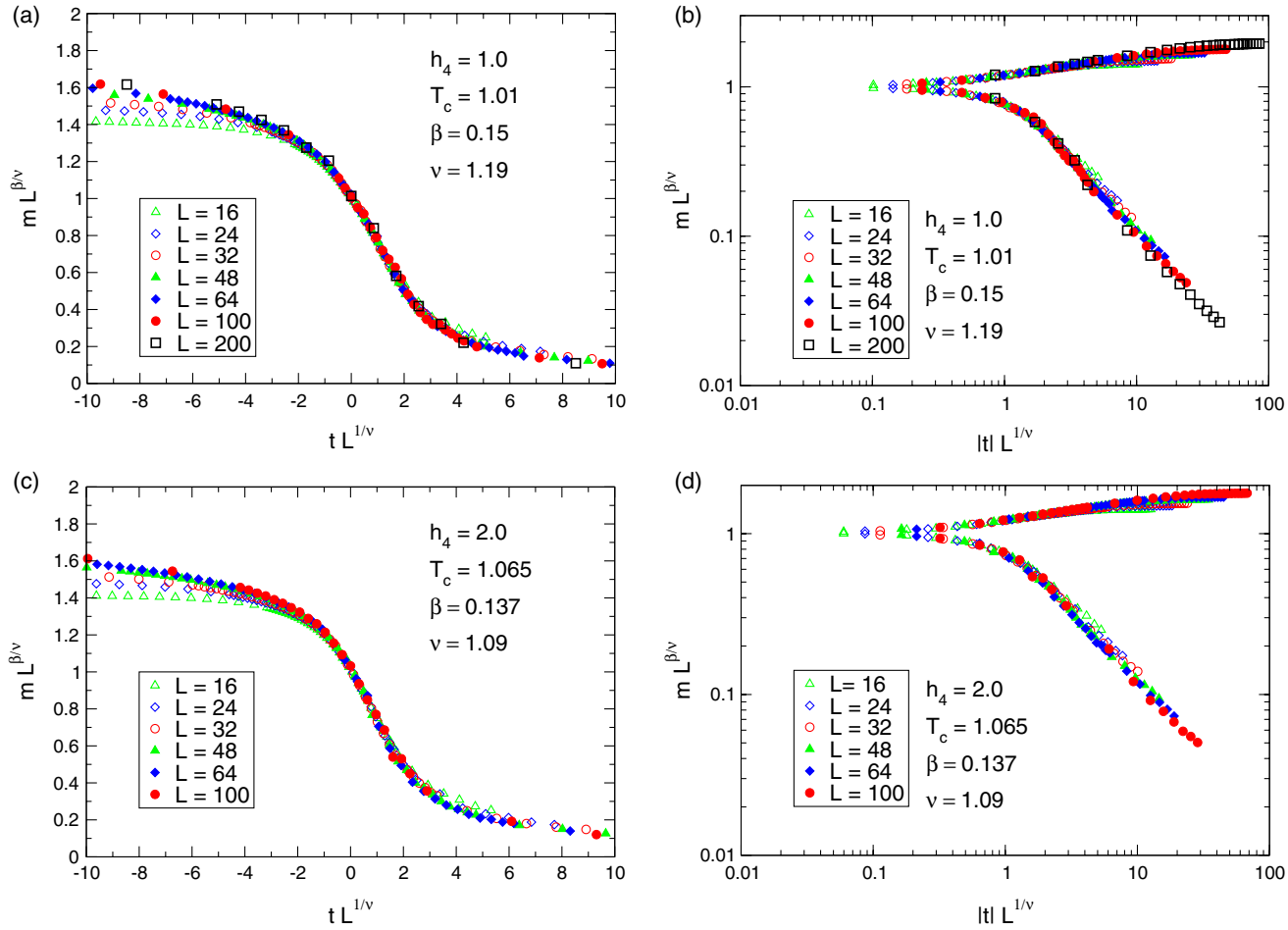

Figure 3. Best data collapses for the 2dXY model with four-fold crystal field $h_4/J = 1.0$ and 2.0 for different system sizes.

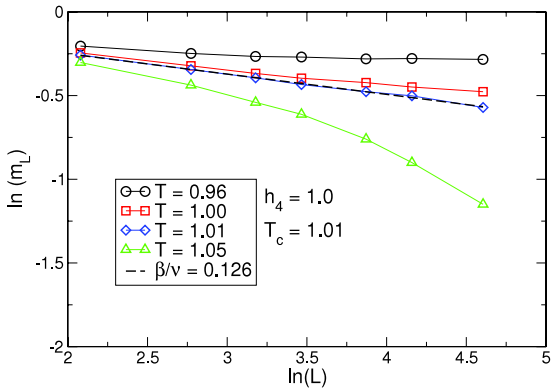

Figure 4. Magnetization m against system size L, on a log–log scale, for the 2dXY model with four-fold crystal field $h_4/J = 1.0$, for temperatures near the transition.

that of the continuous symmetry of the 2dXY model [62], as in the six-fold case. In fact the most detailed finite size scaling analysis [65] shows no evidence of such a crossover for small fields. It therefore remains an open question whether the pocket of pure XY behaviour for small h_4/J is a pragmatic observation related to excessively slow crossover, or whether it remains right to the thermodynamic limit. In either case this is the main result of this section: large values of β are indeed masked by the pocket of 2dXY behaviour, leading to the effective exponent $\tilde{\beta}$ for weak h_4 and creating a divide between systems with strong and weak four-fold fields, with the non-universal character of XYh_4 only appearing for $\beta(h_4) < 0.23$. The threshold value of h_4, separating the two regimes can be estimated theoretically by putting $\beta(h_4) = 0.23$ in equation (6). Using $k_B T_{KT}/J \approx 0.9$ gives $A = 1.6$ and $h_4/J \approx 0.9$, a ratio of order unity, in agreement with the above general arguments, but an over estimate compared with numerics, where the change of regime occurs for $h_4/J \sim 0.5$, corresponding to $A \approx 1$.

Having confirmed that $\eta \approx 0.25$ over the whole range of h_4, we finally fix $\eta = 0.25$ and use our estimates of $\nu(h_4)$ from the scaling collapse to give a further estimate of the exponents as a function of h_4. The estimates of ν and β, summarized in table 2, are in good agreement with all previous unconstrained estimates. We also include estimates of $\beta(T_c^L)$ derived by a typical experimental analysis of fixing T_c^L from the maximum in the susceptibility or where the magnetization approaches zero, and deriving β from a log–log plot. There is seen to be a systematic error between the different estimates of β, especially for small values of h_4. Nevertheless, the experimental exponents are still found to lie in the universal window of values predicted for the 'true' exponents of the underlying model.

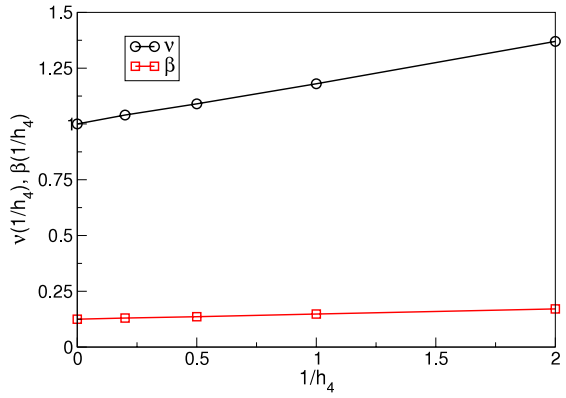

Figure 5. Exponents β and ν measured from a finite size scaling analysis of the Monte Carlo data plotted against $1/h_4$.

Table 2. Critical exponents for the XYh_4 model, as determined from a finite size scaling analysis, and as measured directly from Monte Carlo magnetization data for a system of size $L = 100$.

h_4	ν	β	T_c^L	$\beta(T_c^L)$
0.5	1.37(6)	0.171(10)	1.01(1)	0.214(9)
1	1.19(4)	0.148(5)	1.04(1)	0.196(6)
2	1.09(8)	0.136(10)	1.08(1)	0.155(3)
5	1.04(6)	0.130(7)	1.12(1)	0.129(3)
∞	1.00(5)	0.125(6)	1.14(1)	0.123(3)

The various critical exponents plotted in figure 5 are found to be linear in $1/h_4$. By fitting to $\beta(h_4) = 0.125 + a/h_4$, we estimate the constant a to be 0.032 for the 'true' exponents, and 0.05 for the experimental exponents. These values are clearly very different from those expected for the constant A in equation (6), but once outside the pocket of pure XY behaviour we are no longer in the weak field regime for which equation (6) is valid, as was shown in the previous section.

5. Strong field–weak field divide

Experimental evidence for the strong field–weak field divide comes from making head to head comparisons between systems listed in the appendix.

A quantitative comparison is afforded by the ferromagnet Rb_2CrCl_4 [67] and the antiferromagnet K_2FeF_4 [31], both quasi-two-dimensional square lattice systems with $S = 2$. In both systems the intra-plane isotropic exchange coupling, J, is much bigger than the inter-plane value J', giving rise to an extended temperature range with two-dimensional critical fluctuations. However, while the ferromagnet shows all the characteristics of the pure XY universality class [25, 68], the antiferromagnet has non-universal exponents, with $\beta = 0.15$ [31], which we now see to be consistent with XYh_4. A realistic model Hamiltonian for either system has the following form

$$\mathcal{H} = J_0 \sum_{\langle i,j \rangle} \mathbf{S}_i \cdot \mathbf{S}_j + D \sum_i (S_i^z)^2 + \tfrac{1}{2} e (S_+^4 + S_-^4), \qquad (7)$$

Table 3. Main parameters for K_2FeF_4 and Rb_2CrCl_4, as determined from experiment [31, 67].

	K_2FeF_4	Rb_2CrCl_4
S	2	2
J (K)	−15.7	15.12
D (K)	5.7	1.06
E (K)	−0.49	0.123
$\tilde{D}$	0.363	0.07
$\tilde{e}$	0.0052	0.0013
β	0.15(1)	0.230(2)

where the weak inter-plane exchange and a weak fourth-order axial term are ignored (in the case of Rb_2CrCl_4 small departures from tetragonal symmetry are neglected for the purpose of this discussion).

The crystal field D confines the spins to an easy plane breaking the O(3) rotational symmetry of the Heisenberg exchange and the four-fold term e breaks symmetry within that plane, putting Hamiltonian (7) in the XYh_4 universality class. For both Rb_2CrCl_4 and K_2FeF_4 accurate estimates of the Hamiltonian parameters were derived by fitting magnon dispersions measured by neutron scattering to a self-consistent spin wave calculation [31, 67, 69]. However, in order to fit the spectra, the fourth-order term was decoupled into an effective second-order term, with amplitude $E \approx 6eS^2$. In the low temperature limit one can estimate parameters $\tilde{e} = |eS^4/J_0S^2|$ and $\tilde{D} = |DS^2/J_0S^2|$. Values are shown in table 3 for both materials.

To get an estimate of the four-fold field that determines the critical exponents, it is tempting to assume that systems with $S = 2$ are classical and to associate $\tilde{e}$ with the parameter h_4/J arising from equation (1). The parameter $\tilde{e} = 0.0013$ for Rb_2CrCl_4 and 0.0052 for K_2FeF_4, which seem sufficiently small to put both systems into the weak field regime with pure XY universality, as has been directly confirmed by numerical simulation [70]. However, assigning an effective classical Hamiltonian of the form (1) for systems with finite S is not so straightforward: for finite S, through the uncertainty principle, out-of-plane and in-plane spin fluctuations are not statistically independent. As a consequence the energy scale for in-plane spin rotations and the consequent effective value for h_4 depend collectively on J and D as well as on $\tilde{e}$. This can be seen from a detailed consideration of the magnon dispersion arising from (7). This calculation reveals a distinct difference between the ferromagnetic and antiferromagnetic cases, with the latter retaining strong quantum effects even for $S = 2$. For the antiferromagnet one finds two magnon branches which, for $D = e = 0$, are degenerate and gapless for zero wavevector and where each mode constitutes a conjugate in-plane and out-of-plane spin fluctuation term of equal amplitude. For finite crystal field strength the degeneracy is lifted, energy gaps appear everywhere in the spectrum and the symmetry is broken between the in-plane and out-of-plane fluctuation amplitudes. In the following we refer to a mode as in-plane or out-of-plane if the conjugate variable with the largest amplitude is in or out of the plane. To lowest order in

$1/S$ the out-of-plane branch develops a gap at zero wavevector:

$$\Delta_1 = S\,[2(D+|E|)(2|J|z+4|E|)]^{1/2} \approx 2S\sqrt{Dz|J|}, \quad (8)$$

while the in-plane branch has

$$\Delta_2 = S\,[(4|E|)(2|J|z+2D+2|E|)]^{1/2} \approx 2S\sqrt{2|E|z|J|}, \quad (9)$$

(here $z = 4$). These gaps depend on the geometric mean of the exchange field zJ and the crystal field e or D with the result that they are surprisingly large on the scale of J, as noticed by Thurlings *et al* [31]. For K_2FeF_4 $\Delta_1 = 70.8$ K, $\Delta_2 = 23.9$ K at 4.2 K, renormalizing only weakly with temperature [31]. Δ_1 is larger than the transition temperature, $T_N = 63$ K$\approx JS^2$, so the out-of-plane branch of spin fluctuations will be frozen by quantum effects over the whole of the ordered phase, leaving the predominantly in-plane spin fluctuations only. Interpreting these as the classical fluctuations in an effective plane rotator model with Hamiltonian (1) leads to a crystal field, h_4(eff), of the order of Δ_2. This gives $h_4(\text{eff})/JS^2 \sim 0.33$ which is the right order of magnitude to fall into the strong field category. The fact that for K_2FeF_4, $T_N/JS^2 \approx 1$, as is the case for the model systems with Hamiltonian (1) presented in the previous section, is highly consistent with this interpretation. Higher order terms in $1/S$ renormalize D and $|E|$ such that the values given in table 3 are higher than those predicted by fitting to linear spin wave theory. One can further speculate that quantum fluctuations for the in-plane branch will renormalize the effective h_4 in (1) [64] to an even higher value. The non-universal exponents observed for K_2FeF_4 could therefore be examples of the XYh_4 universality class.

For the ferromagnet Rb_2CrCl_4, D flattens the cone of spin precession, giving a range of q values where the energy spectrum varies approximately linearly with wavevector, but does not open a gap. The field e opens a zero wavevector energy gap that varies as $\sqrt{De}$. It is of order 1 K, decreasing to zero at the transition temperature $T_c = 52$ K, and so can hardly affect the thermodynamics in the critical region. Although the effective value of h_4 depends on the geometric mean of D and e rather than just the bare value of e, it is independent of J and hence much smaller than for the antiferromagnetic case. This places Rb_2CrCl_4 in the weak field regime, consistent with the observation of XY universality for this material [25, 68].

From this comparison, it seems likely that magnetic systems that show true XYh_4 universality will mostly be antiferromagnetic. Indeed a similar 'spin dimensional reduction' due to quantum suppression of fluctuations has recently been observed in quantum Monte Carlo simulations with a Hamiltonian similar to (5) [58]. More calculations beyond the spin wave approximation are required to clarify this point.

Among non-magnetic systems, oxygen absorbed onto Mo(110) [37] or W(110) [71] and hydrogen on W(110) [36] have both been claimed to fall into the XYh_4 class, representing four-fold equivalents of the two-stage melting process for hexagonally coordinated systems [45]. Note that the (110) surface does not have four-fold symmetry, but if we adopt these claims as a premise, then a comparison of the two systems is indeed perfectly consistent with XY h_4 universality and with the preceding arguments about the strong field–weak field divide. Electron hybridization between absorbed and substrate particles will result in the generation of electronic dipoles aligned perpendicularly to the (110) surface. The resulting $1/r^3$ interaction between the particles is repulsive and of sufficiently long range to ensure crystallization into a square lattice. The (110) surface provides a substrate potential with four-fold topology (though not four-fold symmetry) and which can be made commensurate with the free standing array by tuning the adsorbate density, the clearest example being the (2×2) lattice structure [36]. The result is claimed to be in the XYh_4 universality class and the measured exponents, $\beta \simeq 0.19$ [37, 71], are, in light of the current work, consistent with this. In principle, the same should be true for the (2×2) ordering transition for hydrogen on W(110) but the measured β, 0.25, is consistent with the pure XY model [36]. As hydrogen is so much lighter than oxygen, larger zero point fluctuations should make the substrate potential less effective at pinning the crystal, putting it in the category of systems with a weak field h_4, consistent with the experimental observation.

6. Other exponents and scaling relations

Further evidence for the experimental relevance of the finite size effects is found in the behaviour of other critical exponents. The exponent η, which according to the previous weak universality arguments should be 0.25 for all h_4, is only found to closely approximate the theoretical value for model Ising systems such as Rb_2CoF_4 [72]. For model XY systems the predicted $\eta = 0.25$ or $\delta = 15$ are always observed at a temperature *well below* T_c (say 0.9 T_c), with $\eta(T)$ increasing to larger values at T_c, and $\delta(T)$ decreasing, since $\delta = (4-\eta)/\eta$. For example, in the XY layered ferromagnets Rb_2CrCl_4 and K_2CuF_4 $\eta(T)$ and $\delta(T)$ have been measured with precision by several different methods [26, 73, 68]: in both cases η rises to about $\eta = 0.35$ at T_c. This is a very strong signature of the finite size scaling properties of the XY model and is consistent with the predicted logarithmic shift in transition temperature, $[T_c(L) - T_{KT}] \sim \frac{1}{\log^2(L)}$ [21, 51], for a finite size system [74]. As the measured value of η increases continuously through the transition, its value at $T_c(L)$ is thus expected to be in excess of $\eta = 1/4$.

It seems that the anomalous value of $\eta > 0.25$ extends to systems with XYh_4 universality: for example, in K_2FeF_4 it is estimated to be $\eta \approx 0.35$. This is again consistent with the shift in transition temperature observed in finite size systems. Defining $T_c(L)$ from the maximum susceptibility leads to a shift, $[T_c(L) - T_c] \sim L^{-1/\nu}$. Here, in the four-fold field problem, $\nu > 1$ which means that shift remains important even in the intermediate field regime. Referring to figure 4, one can see that extracting a critical exponent from the initial slope, for $T > T_c$, will lead to an overestimate of η. As experiments do not, in general, have access to the finite size scaling information available to numerical studies, it seems reasonable that the experimental η values are generally larger than the expected thermodynamic limit value. Thus, we propose that $\eta(T_c)$ appearing greater that $1/4$ remains a finite size effect.

Similarly, the measured values of ν are systematically smaller than unity, while a consequence of weak universality is that ν should be greater than one for all finite h_4. For example for K_2FeF_4 $\nu \approx 0.9$, giving $\beta/\nu = 0.16$, greater than the predicted ratio $1/8$, but together with $\gamma \approx 1.5$ the set of exponents do satisfy the hyperscaling relation, $2\beta+\gamma = d\nu$, as well as the relation $\beta/\nu = d-2+\eta/2$. The same holds true for oxygen on W(110) [71], for which β and γ have been determined to be 0.19 and 1.48, respectively. The shift in ν is therefore consistent with the shift in η. It seems reasonable to assume that these changes are also due to finite size effects, which at present prevent the observation of the weak universal line we have shown evidence for, for all values of h_4. More detailed experimental and numerical studies to clarify this point would be of great interest.

7. Conclusions

In conclusion, the XY model with four-fold crystal field is of relevance to a great number of experimental two-dimensional systems. We have focused on the largest experimental data sets, those for two-dimensional magnets, adsorbed gaseous monolayers and in particular on the measured exponent β. With regard to the histogram in figure 1, the systems that comprise it can only be fully understood on a case by case basis.

However, we show in this paper that the Hamiltonian (1) contains the principle two-dimensional universality classes that are relevant to experiment and that a uniform distribution of values h_4 would, because of the marginal finite size scaling properties of the model, produce a probability density of the same form as figure 1 with a continuous spectrum bounded by peaks at the Ising and XY limits. This is what we refer to as the universal window for critical exponents. We have further shown that the actual values of the four-fold crystal field that occur in real systems are, at first sight, too small to take any system away from the XY limit. However, we have identified at least one mechanism, in antiferromagnets, whereby the four-fold field is effectively amplified by quantum confinement of the spins to the easy plane. Other mechanisms of realizing XYh_4 universality are possible in individual cases [41, 47]. We have demonstrated the relevance of finite size scaling corrections to the experimental data set, with the relevant length scale giving a crossover away from XY criticality. Future work should focus on the finite size scaling aspects and on individual systems to see if a more accurate quantitative connection between the physical h_4 and the observed critical behaviour can be established. Further to this, we propose here that the non-universal exponents of XYh_4 should satisfy weak universality, with $\beta/\nu = 1/8$ for all h_4 and we have given evidence that this is true in the range of intermediate field values. The robustness of the pocket of true XY behaviour, observed for weak fields [62, 65], in the thermodynamic limit remains an open question. Finally, we remark that all evidence confirms that truly two-dimensional systems, quasi-two-dimensional systems and numerical simulations reveal the same syndrome of behaviour. Consequently, much can be learnt about new two-dimensional systems [2, 3] through comparisons with old ones [31, 67]. It is fortunate that there is such an extensive and carefully determined data base.

Acknowledgments

It is a pleasure to thank Maxime Clusel, Martin Greven, Björgvin Hjörvarsson and Marco Picco for useful discussions. PCWH thanks the London Centre for Nanotechnology and the Royal Society for financial support and the Rudolph Peierls Institute for Theoretical Physics, University of Oxford, for hospitality during the completion of this work. AT thanks the Engineering and Physical Sciences Research Council for a studentship.

Appendix. Construction of the histogram of β exponents

In constructing the histogram of experimental two-dimensional β exponents, a number of factors were considered. First, it was crucial to avoid circular logic by excluding those systems which were assigned a dimensionality purely on the basis of their exponent values, rather than on a large body of experimental evidence. Fortunately, we found no such cases in the literature. Therefore all systems included in the histogram are assigned as two-dimensional on the basis of compelling experimental evidence of two-dimensionality. Likewise we found no examples of systems considered to be two-dimensional that exhibit $\beta \approx 1/3$, which might, in the absence of extra evidence, be mistakenly assigned as three-dimensional systems and wrongly excluded from the data set. It should be noted that in layered magnets, the crossover from two-dimensional to three-dimensional exponents is generally very sharply defined so there is no ambiguity in identifying the two-dimensional regime. A second criterion for inclusion in the histogram was that the exponents were determined with reasonable precision and accuracy (typically $\Delta\beta < \pm 0.01$). This inevitably necessitated a subjective judgement, but only a few results were excluded on these grounds: typically those exponents determined by powder (rather than single crystal) neutron diffraction, which is generally accepted to be inadequate for the accurate determination of β. The experimental exponents are generally not asymptotic exponents, but the numerical study presented above reveals that the difference between asymptotic exponents and those determined using finite size scaling techniques at temperatures down to $\sim 0.9 T_c^L$ is generally negligible at the level of accuracy required for the present purpose. The histogram also excludes a number of interesting systems on the basis of there being legitimate grounds for alternative explanations for their observed critical behaviour. These include metamagnetic materials [75], systems undergoing spin-Peierls transitions [76–78] and bulk systems undergoing order–disorder transitions [79].

The following tables lists all the systems included in the histogram. Table A.1 contains data for layered magnets, and includes examples of molecular magnets [80]. Note that K_2MnF_4 represents two data points in the histogram as the elegant work of van de Kamp *et al* [81] used a magnetic field to tune the system between Ising and XY symmetry, with β

Table A.1. List of two-dimensional critical exponents β for layered magnets reported in the literature, mostly measured by neutron diffraction (F = ferromagnet, A = antiferromagnet, Fo = (HCO_2), chdc = *trans*-1,4-cyclohexanedicarboxylate, 5CAP = 2-amino-5-chloropyridinium, tetren = tetraethylenepentaamine).

System	β	t range	T_c (K)	Type	Reference
Rb_2CoF_4	0.119(8)	1×10^{-1}–2×10^{-4}	102.96	A	[82]
$ErBa_2Cu_3O_7$	0.122(4)	0.11–1×10^{-4}	0.618	A	[83]
K_2CoF_4	0.123(8)	1×10^{-1}–8×10^{-4}	107.85	A	[24]
$BaNi_2(AsO_4)_2$	0.135	3×10^{-1}–1×10^{-2}	19.2	A	[27]
Ba_2FeF_6 [a]	0.135(3)	7×10^{-1}–4×10^{-3}	47.96(4)	A	[84]
K_2NiF_4	0.138(4)	2×10^{-1}–3×10^{-4}	97.23	A	[85]
$K_3Mn_2F_7$	0.154(6)	1×10^{-1}–1×10^{-3}	58.3(2)	A	[86]
Rb_2MnCl_4 ($B < 5.8$ T)	0.15(1)	1×10^{-1}–1×10^{-3}	54	A	[81, 87]
K_2MnF_4	0.15(1)	1×10^{-1}–1×10^{-3}	42.14	A	[88]
K_2FeF_4	0.15(1)	—	63.0(3)	A	[31]
Rb_2MnF_4	0.16(2)	1×10^{-1}–3×10^{-3}	38.4	A	[85]
$Pb_2Sr_2TbCu_3O_8$	0.165(5)	—	5.30(2)	A	[89]
$BaFeF_4$	0.17	3×10^{-1}–1×10^{-2}	54.2	A	[90]
$Cr_2Si_2Te_6$	0.17(1)	6×10^{-1}–3×10^{-2}	32.1(1)	F	[91]
$CsDy(MoO_4)_2$	0.17(1)	—	1.36	A	[92]
$CoCl_2{\cdot}6H_2O$	0.18	4×10^{-1}–4×10^{-2}	2.29	A	[90]
$MnC_3H_7PO_3{\cdot}H_2O$ [b]	0.18(1)	4×10^{-1}–1×10^{-2}	∼15	F	[93]
$MnC_4H_9PO_3{\cdot}H_2O$ [b]	0.18(1)	4×10^{-1}–2×10^{-2}	∼15	F	[93]
$KFeF_4$	0.185(5)	3×10^{-1}–1×10^{-2}	137.2(1)	A	[94, 90]
$Fe(NCS)_2(pyrazine)_2$	0.19(2)	2×10^{-1}–3×10^{-2}	6.8	A	[95]
Rb_2FeF_4	0.2	3×10^{-1}–2×10^{-3}	56.3	A	[85]
La_2CoO_4	0.20(2)	—	274.7(6)	A	[96]
$MnC_2H_5PO_3{\cdot}H_2O$ [b]	0.21(2)	6×10^{-1}–9×10^{-2}	∼15	A	[93]
$NH_4MnPO_4{\cdot}H_2O$ [b]	0.21(3)	8×10^{-1}–2×10^{-2}	17.5(1)	A	[93, 97]
K_2CuF_4	0.22	3×10^{-1}–3×10^{-2}	6.25	F	[98]
$CuFo_2{\cdot}4D_2O$ [c]	0.22(2)	5×10^{-1}–5×10^{-2}	16.72	A	[99]
$CuFo_2{\cdot}CO(ND_2)_2{\cdot}2D_2O$ [c]	0.22(1)	4×10^{-1}–1×10^{-3}	15.31	A	[99]
Tanol suberate [d]	0.22	7×10^{-1}–2×10^{-2}	0.7	F	[100]
$Sr_2CuO_2Cl_2$	0.22(1)	2×10^{-1}–1×10^{-2}	265.5(5)	A	[40]
$MnFo_2{\cdot}2H_2O$	0.22(1)	4×10^{-1}–4×10^{-2}	3.6	A	[101]
La_2NiO_4	0.22(2)	8×10^{-2}–2×10^{-3}	327.5(5)	A	[102]
$BaNi_2(PO_4)_2$	0.23	3×10^{-1}–2×10^{-2}	23.5(5)	A	[27]
$Cu(DCO_2)_2{\cdot}4D_2O$	0.23(1)	$t > 6 \times 10^{-2}$	16.54(5)	A	[103]
Rb_2CrCl_4	0.230(2)	2×10^{-1}–1×10^{-2}	52.3	F	[25]
Gd_2CuO_4	0.23	7×10^{-1}–3×10^{-3}	6.4	A	[104]
$(C_6H_5CH_2NH_3)_2CrBr_4$ [e]	0.23	7×10^{-1}–1×10^{-1}	52.0(1)	F	[105]
$KMnPO_4{\cdot}H_2O$ [b]	0.23(2)	$t > 9 \times 10^{-2}$	∼15	A	[93]
$(CH_3NH_3)_2MnCl_4$	0.23(2)	1×10^{-2}–1×10^{-3}	44.75	F	[106]
$ErCl_3$	0.23(2)	4×10^{-1}–1×10^{-2}	0.350(5)	A	[107]
$(d_6\text{-}5CAP)_2CuBr_4$	0.23(4)	4×10^{-2}–6×10^{-3}	5.18(1)	A	[108]
Li_2VOSiO_4 [d]	0.235(9)	4×10^{-1}–2×10^{-2}	2.85	A	[109]
Li_2VOGeO_4 [d]	0.236	—	1.95	A	[110]
$(tetrenH_5)_{0.8}Cu_4[W(CN)_8]_4{\cdot}7.2H_2O$	0.237(12)	2×10^{-1}–2×10^{-2}	33.16	F	[111]
$La_{0.04}Sr_{2.96}Mn_2O_7$ [d]	0.24(2)	—	145.0(5)	A	[112]
$La_{0.525}Sr_{1.475}MnO_4$	0.24(3)	—	110(1)	A	[113]
$RbFeF_4$	0.245(5)	6×10^{-1}–1×10^{-2}	133(2)	A	[90]
$MnPS_3$	0.25(1)	$t > 3 \times 10^{-2}$	78.6	A	[114, 115]
$Co_5(OH)_8(chdc){\cdot}4H_2O$	0.25(3)	—	60.5	F	[116]
$YBa_2Cu_3O_{6+x}$	0.26(1)	5×10^{-2}–5×10^{-3}	410	A	[117]
Rb_2MnCl_4 ($B > 5.8$ T)	0.26(1)	1×10^{-1}–2×10^{-3}	54	A	[87, 81]
Rb_2CrCl_3Br	0.26(1)	9×10^{-1}–1×10^{-2}	55	F	[118, 119]
$Rb_2CrCl_2Br_2$	0.26(1)	9×10^{-1}–3×10^{-2}	57	F	[118, 119]
$KMnF_4$	0.26(1)	3×10^{-1}–3×10^{-2}	5.2(1)	A	[120]
$RbMnF_4$	0.26(1)	3×10^{-1}–3×10^{-2}	3.7(1)	A	[120]

[a] Studied by Mössbauer spectroscopy.
[b] Studied by bulk magnetometry.
[c] Studied by proton nuclear magnetic resonance (NMR).
[d] Studied by muon spin relaxation (μSR).
[e] Studied by ac susceptibility.

Table A.2. Summary of transition temperatures T_c and magnetization critical exponents β for epitaxial magnetic films grown on a range of substrates. The thickness d_{min} denotes the thickness at which these quantities were measured and t range indicates the range of reduced temperature over which β was measured. The magnetic anisotropy is indicated by the direction of the easy axis, and can either be perpendicular ($\perp$) or parallel ($\parallel$) to the film plane.

System	Structure	d_{min} (ML)	β	t range	T_c (K)	Anisotropy	Method[a]	Reference
Fe on								
Pd(100)	bct, 1 × 1	2.0	0.125(10)	$t < 3 \times 10^{-2}$	613.1	$\perp$	ECS	[121]
		1.2	0.127(4)	1×10^{-1}–3×10^{-3}	<100	$\perp$	MOKE	[122]
Ag(100)	bcc, 1 × 1	2.5–2.7[b]	0.124(2)	1×10^{-1}–1×10^{-3}	324	$\perp$	MOKE	[123, 29]
W(110)	bcc, 1 × 1	0.8	0.124(1)	1×10^{-1}–4×10^{-3}	221.1(1)	$\parallel [1\bar{1}0]$	SPLEED	[124, 4]
		1.0	0.134(3)	1×10^{-1}–5×10^{-2}	224	$\parallel [1\bar{1}0]$	SPLEED	[30]
		1.7	0.13(2)	—	317	$\parallel [1\bar{1}0]$	MOKE	[125]
Ag(111)	bcc, 1 × 1	1.8	0.139(6)	1×10^{-1}–1×10^{-3}	∼450	$\parallel$	MOKE	[126]
		2.0	0.130(3)	1×10^{-1}–1×10^{-3}	∼450	$\parallel$	MOKE	[126]
Cu(100)	fct, 4 × 1	∼2.5[b]	0.17(3)	1×10^{-1}–1×10^{-2}	370	$\perp$[c]	MOKE	[127–129]
W(110)[d]	bcc, 1 × 1	0.82	0.18(1)	3×10^{-1}–1×10^{-2}	282(3)	$\parallel [1\bar{1}0]$	TOM, CEMS	[130–132]
$Cu_{84}Al_{16}$ (100)	fcc, 1 × 1	4.0	0.212(5)	3×10^{-1}–1×10^{-2}	288(2)	$\parallel$	LMDAD	[133]
W(100)	bcc, 1 × 1	1.6	0.217(2)	1×10^{-1}–1×10^{-2}	207.8(1)	$\parallel$ [001]	CEMS, SPLEED	[32, 134]
Au(100)	bcc, 1 × 1	1.0	0.22(1)	1×10^{-1}–1×10^{-3}	300	$\parallel$ [001]	SPLEED	[135]
		2.0	0.25(1)	2×10^{-1}–1×10^{-4}	290	$\parallel$ [001]	ECS	[136]
W(100)[d]	bcc, 1 × 1	1.5	0.22(2)	—	282(1)	$\parallel$ [001]	CEMS	[4]
V(001)	bcc	3	0.23(1)	2×10^{-1}–2×10^{-2}	∼190	$\parallel$	MOKE	[137]
Pd[e]	—	0.2–0.4[b]	0.23(1)	2×10^{-1}–2×10^{-2}	>50	$\parallel$	MOKE	[3]
GaAs(100)	bcc, 2 × 6	3.4	0.26(2)	1×10^{-1}–1×10^{-3}	254.8(2)	$\parallel$	MOKE	[138]
Co on								
Cu(111)	fcc, 1 × 1	1.0	0.125	1×10^{-2}–1×10^{-3}	433	$\perp$	TOM	[139]
		1.5	0.15(8)	—	460	$\perp$	MOKE	[140]
Ni/Pt(111)	fcc	1.0	0.22(2)	—	∼600	$\perp$	MOKE	[141]
Cu(100)	fcc	2.0	0.24	—	∼240	$\parallel$	MOKE	[142, 143]
Ni on								
W(110)	fcc, 7 × 1	2.0	0.13(6)	1×10^{-1}–1×10^{-3}	325	$\parallel$ [001]	FMR	[144]
Co/Pt(111)	fcc	1.0	0.20(2)	—	∼650	$\perp$	MOKE	[141]
Cu(111)	fcc, 1 × 1	2.0–3.0[b]	0.24(7)	3×10^{-1}–6×10^{-3}	380	$\parallel$	MOKE	[145]
Cu(100)	fcc, 1 × 1	4.1	0.23(5)	3×10^{-1}–1×10^{-2}	284	$\parallel$	MOKE	[146, 140]
V on								
Ag(100)	bcc, 1 × 1	5.0	0.128(10)	3×10^{-1}–2×10^{-4}	475.1	$\parallel$ [001]	ECS	[147]
Gd on								
Y(0001)	hcp	1.0	0.23(5)	1×10^{-1}–8×10^{-3}	156	$\parallel$	MOKE	[148]
Mn_5Ge_3 on								
Ge(111)	—	1.0	0.244	2×10^{-1}–4×10^{-3}	296	$\parallel$	SQUID	[149]
$Mn_{0.06}Ge_{0.94}$ on								
Ge(001)	2 × 1	—	0.20(4)	2×10^{-1}–4×10^{-3}	303	$\parallel$	SQUID	[150]
CoAl(100)	bcc, 1 × 1		0.22(2)	2×10^{-1}–7×10^{-3}	∼90	$\parallel$	MOKE	[2]

[a] Experimental properties were measured by the following techniques: electron capture spectroscopy (ECS), magneto-optical Kerr effect (MOKE), spin polarized low energy electron diffraction (SPLEED), torsion oscillation magnetometry (TOM), conversion electron Mössbauer spectroscopy (CEMS), linear magnetic dichroism in the angular distribution of photoelectron intensity (LMDAD) and superconducting quantum interference device (SQUID).

[b] Exponent determined by averaging over values of a range of films of different thickness.

[c] Reversible spin reorientation transition from $\parallel$ to $\perp$ with increasing T.

[d] Coated with Ag.

[e] Pd layers δ-doped with Fe.

recorded for both cases. In all other cases the βs are determined in zero applied field. Table A.2 contains data for ultrathin magnetic films. Although there are several cases in which films of different thicknesses have been measured in order to study crossover to three-dimensional behaviour, only the values of β in the two-dimensional limit are reported here and are included as only one data point in the histogram. Finally, table A.3 includes data for adsorbed gaseous monolayers and systems undergoing surface reconstruction and melting processes.

Our aim has been to make an exhaustive survey up to the time of publication. We apologize to any authors whose work we may have inadvertently overlooked, but we are confident

Table A.3. Chemisorbed and physisorbed systems displaying two-dimensional phase transitions.

System	β	Model ascribed	Method	Reference
$p(2 \times 1)$-O disordering on Ru(001)	0.085(15)	Four-state Potts	LEED	[17]
(3×3)-Sn disordering on Ge(111)	0.11(1)	Three-state Potts	HAS[a], XRD[b]	[34]
Ru(001)$p(2 \times 2)$-S	0.11(2)	Four-state Potts	LEED[c]	[33]
(3×1) reconstruction on Si(113)	0.11(4)	Three-state Potts	LEED	[9]
W(112)$p(2 \times 1)$-O	0.13(1)	2d Ising	LEED	[5]
$p(1 \times 2) \leftrightarrow (1 \times 1)$-Au(110)	0.13(2)	2d Ising	LEED	[6]
$p(2 \times 2)$-O disordering on Ru(001)	0.13(2)	Three-state Potts	LEED	[18]
W(011)$p(2 \times 1)$-H	0.13(4)	2d Ising[d]	LEED	[36]
Ru(001)$(\sqrt{3} \times \sqrt{3})$R30°-S	0.14(3)	Three-state Potts	LEED	[33]
$p(2 \times 2)$-O disordering on Mo(110)	0.19(2)	XYh_4^d	LEED	[37]
$p(2 \times 1)$-O disordering on W(110)	0.19(5)	XYh_4^d	LEED	[71]
Xe melting on graphite	0.23(4)	2dXY	XRD	[8]
W(011)$p(2 \times 2)$-H	0.25(7)	2dXY[d]	LEED	[36]

[a] HAS: helium diffraction.
[b] XRD: x-ray diffraction.
[c] LEED: low energy electron diffraction.
[d] Model not ascribed by original authors.

that these cases would not significantly modify the form of the histogram.

References

[1] Hadzibabic Z, Krüger P, Cheneau M, Battelier B and Dalibard J 2006 Berezinskii–Kosterlitz–Thouless crossover in a trapped atomic gas *Nature* **441** 1118

[2] Rose V, Brüggemann K, David R and Franchy R 2007 Two-dimensional surface magnetism in the bulk paramagnetic intermetallic alloy CoAl(100) *Phys. Rev. Lett.* **98** 037202

[3] Pärnaste M, Marcellini M, Holmström E, Bock N, Fransson J, Eriksson O and Hjörvarsson B 2007 Dimensionality crossover in the induced magnetization of Pd layers *J. Phys.: Condens. Matter* **19** 246213

[4] Elmers H-J 1995 Ferromagnetic monolayers *Int. J. Mod. Phys.* B **9** 3115

[5] Wang G-C and Lu T-M 1985 Physical realization of two-dimensional Ising critical phenomena: oxygen chemisorbed on the W(112) surface *Phys. Rev.* B **31** 5918

[6] Capunzano J C, Foster M S, Jennings G, Willis R F and Unertl W 1985 Au(110) (1×2)-to-(1×1) phase transition: a physical realization of the two-dimensional Ising model *Phys. Rev. Lett.* **54** 2684

[7] Bishop D J and Reppy J D 1978 Study of the superfluid state in two-dimensional ^{4}He films *Phys. Rev. Lett.* **40** 1727

[8] Nuttall W J, Noh D Y, Wells B O and Birgeneau R J 1995 Isothermal melting of near-monolayer xenon on single-crystal graphite *J. Phys.: Condens. Matter* **7** 4337

[9] Yang Y-N, Williams E D, Park R L, Bartelt N C and Einstein T L 1990 Disordering of the (3×1) reconstruction on Si(113) and the chiral three-state Potts model *Phys. Rev. Lett.* **64** 2410

[10] Choy J-H, Kwon S-J and Park G-S 1998 High-T_c superconductors in the two-dimensional limit: $[(\mathrm{Py}\text{–}C_nH_{2n+1})_2HgI_4]$–$Bi_2Sr_2Ca_{m-1}Cu_mO_y$ $(m = 1$ and $2)$ *Science* **280** 1589

[11] Resnik D J, Garland J C, Boyd J T, Shoemaker S and Newrock R S 1981 Kosterlitz–Thouless transition in proximity-coupled superconducting arrays *Phys. Rev. Lett.* **47** 1542

[12] Lapilli C M, Pfeifer P and Wexler C 2006 Universality away from critical points in two-dimensional phase transitions *Phys. Rev. Lett.* **96** 140603

[13] Chung S G 2006 Spontaneous symmetry breaking in Josephson junction arrays *Phys. Lett.* A **355** 394

[14] Trombettoni A, Smerzi A and Sodano P 2005 Observable signature of the Berezinskii–Kosterlitz–Thouless transition in a planar lattice of Bose–Einstein condensates *New J. Phys.* **7** 57

[15] Maier P G and Schwabl F 2004 Ferromagnetic ordering in the two-dimensional dipolar XY model *Phys. Rev.* B **70** 134430

[16] De'Bell K, MacIsaac A B and Whitehead J P 2000 Dipolar effects in magnetic thin films and quasi-two-dimensional systems *Rev. Mod. Phys.* **72** 225

[17] Pfnür H and Piercy P 1989 Critical behaviour of $p(2 \times 1)$ oxygen on Ru(001): an example of four-state Potts critical exponents *Phys. Rev.* B **40** 2515

[18] Pfnür H and Piercy P 1990 Oxygen on Ru(001): critical behaviour of a $p(2\times2)$ order–disorder transition *Phys. Rev.* B **41** 582

[19] Berezinskiĭ V L 1970 Destruction of long-range order in one-dimensional and two-dimensional systems having a continuous symmetry group I. Classical systems *Sov. Phys.—JETP* **32** 493

[20] Kosterlitz J M and Thouless D J 1973 Ordering, metastability and phase transitions in two-dimensional systems *J. Phys. C: Solid State Phys.* **6** 1181

[21] Bramwell S T and Holdsworth P C W 1993 Magnetization and universal sub-critical behaviour in two-dimensional XY magnets *J. Phys.: Condens. Matter* **5** L53

[22] José J V, Kadanoff L P, Kirkpatrick S and Nelson D R 1977 Renormalization, vortices, and symmetry-breaking perturbations in the two-dimensional planar model *Phys. Rev.* B **16** 1217

[23] Calabrese P and Celi A 2002 Critical behaviour of the two-dimensional N-component Landau–Ginzburg Hamiltonian with cubic anisotropy *Phys. Rev.* B **66** 184410

[24] Ikeda H and Hirakawa K 1974 Neutron scattering study of 2-dimensional Ising nature of K_2CoF_4 *Solid State Commun.* **14** 529

[25] Als-Nielsen J, Bramwell S T, Hutchings M T, McIntyre G J and Visser D 1993 Neutron scattering investigation of the static critical properties of Rb_2CrCl_4 *J. Phys.: Condens. Matter* **5** 7871

[26] Hirakawa K 1982 Kosterlitz–Thouless transition in two-dimensional planar ferromagnet K_2CuF_4 *J. Appl. Phys.* **53** 1893

[27] Regnault L P and Rossat-Mignod J 1990 *Magnetic Properties of Layered Transition Metal Compounds* ed L J de Jongh (Dordrecht: Kluwer–Academic) pp 271–321

[28] Bramwell S T and Holdsworth P C W 1993 Universality in two-dimensional magnetic systems *J. Appl. Phys.* **73** 6096

[29] Qiu Z Q, Pearson J and Bader S D 1994 Two-dimensional Ising transition in epitaxial Fe grown on Ag(100) *Phys. Rev.* B **49** 8797

[30] Elmers H-J, Hauschild J and Gradmann U 1996 Critical behavior of the uniaxial ferromagnetic monolayer Fe(110) on W(110) *Phys. Rev.* B **54** 15224

[31] Thurlings M P H, Frikkee E and de Wijn H W 1982 Spin-wave analysis in the two-dimensional antiferromagnet K_2FeF_4. I. Neutron scattering *Phys. Rev.* B **25** 4750

[32] Elmers H-J, Hauschild J, Liu G H and Gradmann U 1996 Critical phenomena in the two-dimensional XY magnet Fe(100) on W(100) *J. Appl. Phys.* **79** 4984

[33] Sokolowski M and Pfnür H 1994 Continuous order–disorder phase transitions of the $p(2 \times 2)$ and $p(\sqrt{3} \times \sqrt{3})$R30° superstructures of sulfur on Ru(001): effective critical exponents and finite size effects *Phys. Rev.* B **49** 7716

[34] Floreano L, Cvetko D, Bavdek G, Benes M and Morgante A 2001 Order–disorder transition of the (3×3) Sn/Ge(111) phase *Phys. Rev.* B **64** 075405

[35] Rau C and Robert M 1996 Anisotropic XY model for two-dimensional Fe *Mod. Phys. Lett.* B **10** 223

[36] Lyuksyutov I F and Fedorus A G 1981 Critical exponents of the H–W(011) system *Sov. Phys.—JETP* **53** 1317

[37] Grzelakowski K, Lyuksyutov I and Bauer E 1990 Direct observation of scaling by high-resolution low-energy electron diffraction: O on Mo(110) *Phys. Rev. Lett.* **64** 32

[38] Lancaster T *et al* 2007 Intrinsic magnetic order in Cs_2AgF_4 detected by muon-spin relaxation *Phys. Rev.* B **75** 220408

[39] Rønnow H M, McMorrow D F and Harrison A 1999 High-temperature magnetic correlations in the 2D $S = 1/2$ antiferromagnet copper formate tetradeuterate *Phys. Rev. Lett.* **82** 3152

[40] Greven M, Birgeneau R J, Endoh Y, Kastner M A, Matsuda M and Shirane G 1995 Neutron scattering study if the two-dimensional spin $S = 1/2$ square-lattice Heisenberg antiferromagnet $Sr_2CuO_2Cl_2$ *Z. Phys.* B **96** 465

[41] Prakash S and Henley C L 1990 Ordering due to disorder in dipolar magnets on two-dimensional lattices *Phys. Rev.* B **42** 6574

[42] De'Bell K, MacIsaac A B, Booth I N and Whitehead J P 1997 Dipolar-induced planar anisotropy in ultrathin magnetic films *Phys. Rev.* B **55** 15108

[43] Carbognani A, Rastelli E, Regina S and Tassi A 2000 Dipolar interaction and long-range order in the square planar rotator model *Phys. Rev.* B **62** 1015

[44] Fernández J F and Alonso J J 2007 Nonuniversal critical behavior of magnetic dipoles on a square lattice *Phys. Rev.* B **76** 014403

[45] Nelson D R and Halperin B I 1979 Dislocation-mediated melting in two dimensions *Phys. Rev.* B **19** 2457

[46] Schick M 1981 The classification of order–disorder transitions on surfaces *Prog. Surf. Sci.* **11** 245

[47] Landau D P and Binder K 1985 Phase diagrams and critical behavior of Ising square lattices with nearest-, next-nearest-, and third-nearest-neighbor couplings *Phys. Rev.* B **31** 5946

[48] Huse D A and Fisher M E 1982 Domain walls and the melting of commensurate surface phases *Phys. Rev. Lett.* **49** 793

[49] Betts D D 1964 Exact solution of some lattice statistics models with 4 states per site *Can. J. Phys.* **42** 1564

[50] Villain J 1975 Theory of one- and two-dimensional magnets with an easy magnetisation plane. II. The planar, classical, two-dimensional magnet *J. Physique* **36** 581

[51] Kosterlitz J M 1974 The critical properties of the two-dimensional XY model *J. Phys. C: Solid State Phys.* **7** 1046

[52] José J V, Kadanoff L P, Kirkpatrick S and Nelson D R 1978 Renormalization, vortices, and symmetry-breaking perturbations in the two-dimensional planar model *Phys. Rev.* B **17** 1477 (erratum)

[53] Plischke M and Bergersen B 1994 *Equilibrium Statistical Physics* 2nd edn (London: World Scientific)

[54] Suzuki M 1974 New universality of critical exponents *Prog. Theor. Phys.* **51** 1992

[55] Baxter R J 1982 *Exactly Solved Models in Statistical Mechanics* (London: Academic)

[56] Janke W and Nather K 1991 Numerical evidence for Kosterlitz–Thouless transition in the 2D XY Villain model *Phys. Lett.* A **157** 11

[57] Chung S G 1999 Essential finite-size effect in the two-dimensional XY model *Phys. Rev.* B **60** 11761

[58] Cuccoli A, Roscilde T, Vaia R and Verrucchi P 2003 Detection of XY behaviour in weakly anisotropic quantum antiferromagnets on the square lattice *Phys. Rev. Lett.* **90** 167205

[59] Zhou C, Landau D P and Schulthess T C 2007 Monte Carlo simulations of Rb_2MnF_4: a classical Heisenberg antiferromagnet in two dimensions with dipolar interaction *Phys. Rev.* B **76** 024433

[60] Hikami S and Tsuneto T 1980 Phase transition of quasi-two dimensional planar system *Prog. Theor. Phys.* **63** 387

[61] Mermin N D and Wagner H 1966 Absence of ferromagnetism or antiferromagnetism in one- or two-dimensional isotropic Heisenberg models *Phys. Rev. Lett.* **17** 1133

[62] Bramwell S T, Holdsworth P C W and Rothman J 1997 Magnetization in ultrathin films: critical exponent β for the 2D XY model with four-fold crystal fields *Mod. Phys. Lett.* B **11** 139

[63] Binder K 1981 Critical properties from Monte Carlo coarse graining renormalization *Phys. Rev. Lett.* **47** 693

[64] Rastelli E, Regina S and Tassi A 2004 Monte Carlo simulation for square planar model with small four fold symmetry-breaking field *Phys. Rev.* B **70** 174447

[65] Rastelli E, Regina S and Tassi A 2004 Monte Carlo simulation of a planar rotator model with symmetry-breaking fields *Phys. Rev.* B **69** 174407

[66] Schneider T and Stoll E 1976 Molecular-dynamics study of a two-dimensional ferrodistortive XY model with quartic anisotropy *Phys. Rev. Lett.* **36** 1501

[67] Hutchings M T, Als-Nielsen J, Lindgard P A and Walker P J 1981 Neutron scattering investigation of the temperature dependence of long-wavelength spin waves in ferromagnetic Rb_2CrCl_4 *J. Phys. C: Solid State Phys.* **14** 5327

[68] Bramwell S T, Holdsworth P C W and Hutchings M T 1995 Static and dynamic magnetic properties of Rb_2CrCl_4: ideal 2D-XY behaviour in a layered magnet *J. Phys. Soc. Japan.* **64** 3066

[69] Oguchi T 1960 Theory of spin-wave interactions in ferro- and antiferromagnetism *Phys. Rev.* **117** 117

[70] Taroni A 2007 Theoretical investigations of two-dimensional magnets *PhD Thesis* University College London

[71] Baek D H, Chung J W and Han W K 1993 Critical behaviour of the $p(2 \times 1)$-O/W(110) system *Phys. Rev.* B **47** 8461

[72] Ikeda H, Suzuki M and Hutchings M T 1979 Neutron scattering investigation of static critical phenomena in the two-dimensional antiferromagnets: $Rb_2Co_cMg_{1-c}Cl_4$ *J. Phys. Soc. Japan* **46** 1153

[73] Cornelius C A, Day P, Fyne P J, Hutchings M T and Walker P J 1986 Temperature and field dependence of the magnetisation of Rb_2CrCl_4: a two-dimensional easy-plane ionic ferromagnet *J. Phys. C: Solid State Phys.* **19** 909

[74] Cardy J 1996 *Scaling and Renormalization in Statistical Physics* (Cambridge: Cambridge University Press)

[75] Rujiwatra A, Kepert C J, Claridge J B, Rosseinsky M J, Kumagai H and Kurmoo M 2001 Layered cobalt hydroxysulfates with both rigid and flexible organic pillars: synthesis, porosity and cooperative magnetism *J. Am. Chem. Soc.* **123** 10584

[76] Gaulin B D, Lumsden M D, Kremer R K, Lumsden M A and Dabkowska H 2000 Two dimensional ordering and fluctuations in α'-NaV_2O_5 *Phys. Rev. Lett.* **84** 3446

[77] Lorenzo J E *et al* 1999 Observation of a Kosterlitz–Thouless state at the spin-Peierls phase transition in $CuGuO_3$ *Europhys. Lett.* **45** 45

[78] Birgeneau R J, Kiryukhin V and Wang Y J 1999 Tricritical to mean-field crossover at the spin-Peierls transition in $CuGeO_3$ *Phys. Rev.* B **60** 14816

[79] Harris M J 1999 A new explanation for the unusual critical behaviour of calcite and sodium nitrate, $NaNO_3$ *Am. Mineral.* **84** 1632

[80] Blundell S J and Pratt F L 2004 Organic and molecular magnets *J. Phys.: Condens. Matter* **16** R771

[81] van de Kamp R, Steiner M and Tietze-Jaensch H 1998 Study of the phase diagram and the critical behaviour of the 2D Heisenberg antiferromagnet with small uniaxial anisotropy *Physica* B **241** 570

[82] Samuelsen E J 1973 Experimental study of the two-dimensional Ising antiferromagnet Rb_2CoF_4 *Phys. Rev. Lett.* **31** 936

[83] Lynn J W, Clinton T W, Li W-H, Erwin R W, Liu J Z, Vandervoort K and Shelton R N 1989 2D and 3D magnetic behavior of Er in $ErBa_2Cu_3O_7$ *Phys. Rev. Lett.* **63** 2606

[84] Brennan K, Hohenemser C and Eibschütz M 1993 2D and 3D magnetic behavior of Er in $ErBa_2Cu_3O_7$ *J. Appl. Phys.* **73** 5500

[85] Birgeneau R J, Guggenheim H J and Shirane G 1970 Neutron scattering investigation of phase transitions and magnetic correlations in the two-dimensional antiferromagnets K_2NiF_4, Rb_2MnF_4, Rb_2FeF_4 *Phys. Rev.* B **1** 2211

[86] van Uijen C M J, Frikkee E and de Wijn H W 1979 Neutron scattering study of magnetic ordering in the double-layer antiferromagnet $K_3Mn_2F_7$ *Phys. Rev.* B **19** 509

[87] Tietze-Jaensch H, van de Kamp R and Schmidt W 1998 Magnetic excitation mode splitting and finite size effects in Rb_2MnCl_4 *Physica* B **241** 566

[88] Birgeneau R J, Guggenheim H J and Shirane G 1973 Spin waves and magnetic ordering in K_2MnF_4 *Phys. Rev.* B **8** 304

[89] Wu S Y, Li W-H, Lee K C, Lynn J W, Meen T H and Yang H D 1996 Two- and three-dimensional magnetic correlations of Tb in $Pb_2Sr_2TbCu_3O_8$ *Phys. Rev.* B **54** 10019

[90] de Jongh L J and Miedema A R 1974 Experiments on simple magnetic model systems *Adv. Phys.* **23** 6

[91] Carteaux V, Moussa F and Spiesser M 1995 2d Ising-like ferromagnetic behaviour for the lamellar $Cr_2Si_2Te_6$ compound: a neutron scattering investigation *Europhys. Lett.* **29** 245

[92] Khatsko E N, Zheludev A, Tranquada J M, Clooster W T, Knigavko A M and Srivastava R C 2004 Neutron scattering study of the layered Ising magnet $CsDy(MoO_4)_4$ *Low. Temp. Phys.* **30** 133

[93] Carling S G, Day P and Visser D 1995 Dimensionality crossovers in the magnetization of the weakly ferromagnetic two-dimensional manganese alkylphosphonate hydrates $MnC_nH_{2n+1}PO_3{\cdot}H_2O$, $n = 2$–4 *J. Phys.: Condens. Matter* **7** L109

[94] Eibschütz M L, Guggenheim H J, Holmes L and Burnstein J L 1972 $CsFeF_4$: a new planar antiferromagnet *Solid State Commun.* **11** 457

[95] Bordallo H N, Chapon L, Manson J L, Hernàndez-Velasco J, Ravot D, Reiff W M and Arhyriou D N 2004 $S = 1/2$ Ising behavior in the two-dimensional molecular magnet $Fe(NCS)_2(pyrazine)_2$ *Phys. Rev.* B **69** 224405

[96] Yamada K, Matsuda M, Endoh Y, Keimer B, Birgeneau R J, Onodera S, Mizusaki J, Matsuura T and Shirane G 1989 Successive antiferromagnetic phase transitions in single-crystal La_2CoO_4 *Phys. Rev.* B **39** 2336

[97] Carling S G, Day P and Visser D 1993 Dimensionality crossovers in the magnetization of the canted antiferromagnets $NH_4MnPO_4{\cdot}H_2O$ *Solid State Commun.* **88** 135

[98] Hirakawa K and Ikeda K 1973 Investigation of two-dimensional ferromagnet K_2CuF_4 by neutron scattering *J. Phys. Soc. Japan* **35** 1328

[99] Koyama K, Nobumasa H and Matsuura M 1987 Spontaneous staggered magnetization of two-dimensional Heisenberg like antiferromagnet with canting interaction *J. Phys. Soc. Japan* **56** 1553

[100] Blundell S J, Hausmann A, Jestädt Th, Pratt F L, Marshall I M, Lovett B W, Kurmoo M, Sugano T and Hayes W 2000 Muon studies of molecular magnetism *Physica* B **289** 115

[101] Matsuura M, Koyama K and Murakami Y 1985 Asymmetric critical phenomena in a quasi two-dimensional-Heisenberg antiferromagnet $Mn(HCCO)_2{\cdot}H_2O$ and $Rb_2CrCl_2Br_2$ *J. Phys. Soc. Japan* **54** 2714

[102] Nakajiama K, Yamada K, Hosoya S, Endoh Y, Greven M and Birgeneau R J 1995 Spin dynamics and spin correlations in the spin $S = 1$ two-dimensional square-lattice Heisenberg antiferromagnet La_2NiO_4 *Z. Phys.* B **96** 479

[103] Clarke S J, Harrison A, Mason T E, McIntyre G J and Visser D 1992 Magnetic ordering and fluctuations in the $S = 1/2$ square Heisenberg antiferromagnet $Cu(DCO_2)_2{\cdot}4D_2O$ *J. Phys.: Condens. Matter* **4** L71

[104] Chattopadhyay T, Brown P J, Stepanov A A, Zvyagin A I, Barilo S N and Zhigunov D I 1992 Antiferromagnetic ordering in Gd_2CuO_4 *J. Magn. Magn. Mater.* **104** 607

[105] Bellitto C, Filaci P and Patrizio S 1987 Zero-field magnetic susceptibility study of the magnetic phase transition in the two-dimensional ionic ferromagnet bis(benzylammonium) tetrabromochromate(II), $(C_6H_5CH_2NH_3)_2CrBr_4$ *Inorg. Chem.* **26** 191

[106] Paduan-Filho A and Becerra C C 2002 Magnetic properties and critical behavior of the pure and diluted two-dimensional weak ferromagnet $(CH_3NH_3)_2Mn_{1-x}Cd_xCl_4$ *J. Appl. Phys.* **91** 8294

[107] Krämer K W, Güdel H U, Fischer P, Fauth F, Fernandez-Diaz M T and Hauß T 2000 Triangular antiferromagnetic order in the honeycomb layer lattice of $ErCl_3$ *Eur. Phys. J.* B **18** 39

[108] Coomer F C *et al* 2007 Neutron diffraction studies of nuclear and magnetic structures in the $S = 1/2$ square Heisenberg antiferromagnets $(d_6\text{-}5CAP)_2CuX_4$ (X = Br and Cl) *Phys. Rev.* B **75** 094424

[109] Melzi R, Aldrovandi S, Tedoldi F, Carretta P, Millet P and Mila F 2001 Magnetic and thermodynamic properties of Li_2VOSiO_4: a two-dimensional $S = 1/2$ frustrated antiferromagnet on a square lattice *Phys. Rev.* B **64** 024409

[110] Carretta P, Papinutto N, Melzi R, Millet P, Gonthier S, Mendels P and Wzietek P 2004 Magnetic properties of frustrated two-dimensional $S = 1/2$ antiferromagnets on a square lattice *J. Phys.: Condens. Matter* **16** S849

[111] Pratt F L, Zieliński P M, Bałanda M, Podgajny R, Wasiutyński T and Sieklucka B 2007 A μSR study of magnetic ordering and metamagnetism in a bilayered molecular magnet *J. Phys.: Condens. Matter* **19** 456208

[112] Coldea A I, Blundell S J, Steer C A, Mitchell J F and Pratt F L 2002 Spin freezing and magnetic inhomogeneities in bilayer manganites *Phys. Rev. Lett.* **89** 177601

[113] Larochelle S, Mehta A, Lu L, Mang P K, Vajk O P, Kaneko N, Zhou L and Greven M 2005 Structural and magnetic properties of the single-layer manganese oxide $La_{1-x}Sr_{1+x}MnO_4$ *Phys. Rev.* B **71** 024435

[114] Rønnow H M, Wildes A R and Bramwell S T 2000 Magnetic correlations in the 2D $S = \frac{5}{2}$ honeycomb antiferromagnet $MnPS_3$ *Physica* B **276** 676

[115] Wildes A R, Rønnow H M, Roessli B, Harris M J and Godfrey K W 2006 Static and dynamic critical properties of the quasi-two-dimensional antiferromagnet $MnPS_3$ *Phys. Rev.* B **74** 094422

[116] Kurmoo M, Kaumagai H, Hughes S M and Kepert C J 2003 Reversible guest exchange and ferrimagnetism ($T_c = 60.5$ K) in a porous cobalt(II)-hydroxide layer structure pillared with *trans*-1,4-cyclohexanedicarboxylate *Inorg. Chem.* **42** 6709

[117] Montfrooij W, Casalta H, Schleger P, Andersen N H, Zhokiv A A and Christiansen A N 1998 Dimensional crossover in the XY-compound $YBa_2Cu_3O_{3+x}$ *Physica* B **241–243** 848

[118] Bramwell S T 1989 Neutron scattering, magnetometry and optical spectroscopy of Rb_2CrCl_4, Rb_2CrCl_3Br, $Rb_2CrCl_2Br_2$ and $Rb_2CrCl_2I_2$ *PhD Thesis* University of Oxford

[119] Bramwell S T, Day P, Hutchings M T, Thorne J R G and Visser D 1986 Neutron scattering and optical study of the magnetic properties of the two-dimensional ionic ferromagnets Rb_2CrCl_3Br and $Rb_2CrCl_2Br_2$ *Inorg. Chem.* **25** 417

[120] Morón M C, Palacio F and Rodriguez-Carvajal J 1993 Crystal and magnetic structures of $RbMnF_4$ and $KMnF_4$ investigated by neutron powder diffraction: the relationship between structure and magnetic properties in the Mn^{3+} layered perovskites $AMnF_4$ (A = Na, K, Rb, Cs) *J. Phys.: Condens. Matter* **5** 4909

[121] Rau C, Mahavadi P and Lu M 1993 Magnetic order and critical behavior at surfaces of ultrathin Fe(100) $p(1\times1)$ films on Pd(100) substrates *J. Appl. Phys.* **73** 6757

[122] Liu C and Bader S D 1990 Two-dimensional magnetic phase transition of ultrathin iron films on Pd(100) *J. Appl. Phys.* **67** 5758

[123] Qiu Z Q, Pearson J and Bader S D 1993 Asymmetry of the spin reorientation transition in ultrathin Fe films and wedges grown on Ag(100) *Phys. Rev. Lett.* **70** 1006

[124] Elmers H-J, Hauschild J, Höche H, Gradmann U, Bethge H, Heuer D and Köhler U 1994 Submonolayer magnetism of Fe(110) on W(110): finite width scaling of stripes and percolation between islands *Phys. Rev. Lett.* **73** 898

[125] Back C H, Würsch Ch, Vaterlaus A, Ramsperger U, Maier U and Pescia F 1995 Experimental confirmation of universality for a phase transition in two dimensions *Nature* **378** 597

[126] Qiu Z Q, Pearson J and Bader S D 1991 Magnetic phase transition of ultrathin Fe films on Ag(111) *Phys. Rev. Lett.* **67** 1646

[127] Li D, Freitag M, Pearson J, Qiu Z Q and Bader S D 1994 Magnetic phases of ultrathin Fe grown on Cu(100) as epitaxial wedges *Phys. Rev. Lett.* **72** 3112

[128] Thomassen J, May F, Felfmann B, Wuttig M and Ibach H 1992 Magnetic live surface layers in Fe/Cu(100) *Phys. Rev. Lett.* **69** 3831

[129] Pappas D P, Kämper K-P and Hopster H 1990 Reversible transition between perpendicular and in-plane magnetization in ultrathin films *Phys. Rev. Lett.* **64** 3179

[130] Gradmann U, Przybylski M, Elmers H-J and Liu G 1989 Ferromagnetism in the thermodynamically stable monolayer Fe(110) on W(110), coated by Ag *Appl. Phys.* A **49** 563

[131] Przybylski M and Gradmann U 1987 Ferromagnetic order in a Fe(110) monolayer on W(110) by Mössbauer spectroscopy *Phys. Rev. Lett.* **59** 1152

[132] Elmers H-J, Liu G and Gradmann U 1989 Magnetometry of the ferromagnetic monolayer Fe(110) on W(110) coated with Ag *Phys. Rev. Lett.* **63** 566

[133] Macedo W A A, Sirotti F, Panaccione G, Schatz A, Keune W, Rodrigues W N and Rossi G 1998 Magnetism of atomically thin fcc Fe overlayers on an expanded fcc lattice: $Cu_{84}Al_{16}$ (100) *Phys. Rev.* B **58** 11534

[134] Elmers H-J and Hauschild J 1994 Magnetism and growth in psudomorphic Fe films on W(100) *Surf. Sci.* **320** 134

[135] Dürr W, Taborelli M, Paul O, Germar R, Gudat W, Pescia D and Landolt M 1989 Magnetic phase transition in two-dimensional ultrathin Fe films on Au(100) *Phys. Rev. Lett.* **62** 206

[136] Rau C 1989 Ferromagnetic order and critical behaviour at surfaces of ultrathin epitaxial films *Appl. Phys.* A **49** 579

[137] Pärnaste M, Marcellini M and Hjörvarsson B 2005 Oscillatory exchange coupling in the two-dimensional limit *J. Phys.: Condens. Matter* **17** L477

[138] Bensch F, Garreau G, Moosbühler R, Bayreuther G and Beaurepaire E 2001 Onset of ferromagnetism on Fe epitaxially grown on GaAs(001) (4×2) and (2×6) *J. Appl. Phys.* **89** 7133

[139] Kohlepp J, Elmers H-J, Cordes S and Gradmann U 1992 Power laws of magnetization in ferromagnetic monolayers and the two-dimensional Ising model *Phys. Rev.* B **45** 12287

[140] Huang F, Kief M T, Mankey G J and Willis R F 1994 Magnetism in the few monolayer limit: a surface magneto-optic kerr-effect study of the magnetic behavior of ultrathin films of Co, Ni, and Co–Ni alloys on Cu(100) and Cu(111) *Phys. Rev.* B **49** 3962

[141] Ho H Y, Chen Y J, Hwang E J, Yu S K and Shern C S 2007 Depression of Curie temperature by surface structural phase transition *Appl. Phys. Lett.* **90** 142505

[142] Kuo C C, Chiu C L, Lin W C and Lin M-T 2002 Dramatic depression of Curie temerature for magnetic Co/Cu(100) ultrathin films upon deposition at elevated temperature *Surf. Sci.* **520** 121

[143] Gruyters M, Bernhard T and Winter H 2005 Structural effects on the magnetix behaviour of ultrathin Co films on Cu(001) at the T_c jump *J. Magn. Magn. Mater.* **292** 192

[144] Li Y and Baberschke K 1992 Dimensional crossover in ultrathin Ni(111) films on W(110) *Phys. Rev. Lett.* **68** 1208

[145] Ballantine C A, Fink R L, Araya-Pochet J and Erskine J L 1990 Magnetic phase transition in a two-dimensional system: $p(1\times1)$-Ni on Cu(111) *Phys. Rev.* B **41** 2631

[146] Huang F, Mankey G J, Kief M T and Willis R F 1993 Finite-size scaling behaviour of ferromagnetic thin films *J. Appl. Phys.* **73** 6760

[147] Rau C, Xing G and Robert M 1988 Ferromagnetic order and critical behavior at surfeces of ultrathin V(100) $p(1\times1)$ films on Ag(100) *J. Vac. Sci. Technol.* A **6** 579

[148] Gajdzik M, Trappmann T, Sürgers C and Löhneysen H v 1998 Morphology and magnetic properties of submonolayer Gd films *Phys. Rev.* B **57** 3525

[149] Zeng C, Erwin S C, Feldman L C, Li A P, Jin R, Song Y, Thompson J R and Weitering H H 2003 Epitaxial ferromagnetic Mn_5Ge_3 on Ge(111) *Appl. Phys. Lett.* **83** 5002

[150] De Padova P *et al* 2008 $Mn_{0.06}Ge_{0.94}$ diluted magnetic semiconductor epitaxially grown on Ge(001): influence of Mn_5Ge_3 nanoscopic clusters on the electronic and magnetic properties *Phys. Rev.* B **77** 045203